# Enhancement of Strength and Superplasticity in a 6061 Al Alloy Processed by Equal-Channel-Angular-Pressing

W.J. KIM, J.K. KIM, T.Y. PARK, S.I. HONG, D.I. KIM, Y.S. KIM, and J.D. LEE

Pre–equal-channel-angular-pressing (ECAP) solution treatment combined with post–ECAP aging treatment has been found to be effective in enhancing the room-temperature strength of 6061 aluminum alloy. The largest increase in ultimate tensile strength (UTS) (=460 MPa) and yield stress (YS) (=425 MPa) is obtained in post–ECAP aged 6061 Al with six pressings. The strength increases by a factor of 1.4 when compared to T6 treated commercial 6061 Al. The strength of 6061 Al obtained in the present research is higher than that of ECA-pressed 6061 Al with pre–ECAP peak-aging treatment studied by other investigators. The more effective strengthening of post–ECAP low-temperature aging may be linked with the higher dislocation accumulation rate in the solutionized matrix and the presence of higher density particles in the aged matrix. Modest low-temperature (523 K) and high-temperature (813 K) superplasticity is observed in the ECAP 6061 Al, which may be a result of increased grain boundary area from grain refinement.

## I. INTRODUCTION

EQUAL-CHANNEL-ANGULAR-PRESSING (ECAP) provides a technique for producing microstructures with ultra-fine grain sizes in the submicrometer or nanometer range in bulk materials by introducing extremely large plastic straining during deformation processing.[1–6] The ECAP is accompanied by pressing a billet of material through a die having two equal area channels that intersect at an angle. A billet experiences simple shear without change in cross-sectional area upon passage through such a die and so the process is amenable to repetition. This procedure is particularly interesting, since it can be applied to commercial cast alloys with coarse microstructure to fabricate ultra-fine grained bulk materials that have a low level of porosity, high strength at low temperatures, and superplastic properties at high temperatures.

A 6061 Al is one of the commercial aluminum alloys being massively used in aerospace and automobile industries; its advantages include good formability, fairly good corrosion resistance, weldability, and lower cost compared to 2xxx and 7xxx alloys. Furthermore, since this alloy is heat treatable, it can be strengthened appreciably during aging. The ECAP technique combined with pre–ECAP heat treatment has been applied to 6061 Al to improve its strength at room temperature.[7] Ferrasse *et al.*[7] studied the effect of pre–ECAP heat treatment (*i.e.*, peak-aging and overaging) on development of submicrostructure in the ECAP-processed 6061 Al. They found that the ECAP-processed peak-aged material exhibited much higher strength than the ECAP-processed overaged material, although both materials had similar subgrain sizes of ~0.4 $\mu$m. The increase in strength after ECAP, however, was more pronounced in the overaged material (*i.e.*, 180 pct) compared to the peak-aged material (*i.e.*, 15 pct). They[7] attributed this result to differences in the primary obstacles to dislocation motion. In the peak-aged state, fine precipitate particles formed during aging serve more efficiently as obstacles to plastic flow than new dislocations created during the ECAP process, while the new dislocations are more effective than the precipitate particles, which are coarser and less dense in the overaged state.[7]

The present study has two objectives. One is applying post–ECAP aging treatment rather than pre–ECAP heat treatment adopted by Ferrasse *et al.*[7] to improve the room-temperature strength of commercial 6061 Al. Before the ECAP process, the alloy was solid-solution treated and quenched into water; after the ECAP process, the material was aged at relatively low temperatures. Tensile properties of the ECAP-processed 6061 Al with post–ECAP aging were compared with an ordinary peak-aged T6 6061 Al in terms of yield stress, ultimate tensile strength, and tensile elongation-to-failure.

The other goal of this study is to explore the possibility of superplasticity in ECAP-processed 6061 Al. Extensive research has been devoted to the development of fine-grained, superplastic 2xxx, 5xxx, and 7xxx alloys by static or dynamic recrystallization. In contrast, relatively few studies have been undertaken on superplasticity in 6xxx alloys. Though there is a report of the success on superplasticity in a 6013 alloy with a relatively high Cu content using a method of particle-stimulated nucleation of recrystallization[8] and in a 6061 alloy fabricated using powder metallurgy,[9] no superplasticity has been reported in an ingot-processed 6061 alloy.[10]

## II. EXPERIMENTAL PROCEDURE

A conventionally extruded 6061 Al with a chemical composition of 0.56 pct Si-0.22 pct Fe-0.24 pct Cu-0.02 pct Mn-1.01 pct Mg-0.01 pct Zn-0.06 pct Cr-balance Al in weight

W.J. KIM, Professor, and J.K. KIM and T.Y. PARK, Students, are with the Department of Metallurgy and Materials Science, Hong-Ik University, Seoul 121-7941, Korea. Contact e-mail: kimwj@wow.hongik.ac.kr S.I. HONG, Professor, is with the Department of Metallurgical Engineering, Chungnam National University, Taejeon 305-764, Korea. D.I. KIM, Professor, is with the Department of Materials Science and Engineering, Kunsan National University, Jeollabuk-do 573-701, Korea. Y.S. KIM, Professor, is with the School of Metallurgical and Material Engineering, Kookmin University, Seoul 136-702, Korea. J.D. LEE, Researcher, is with the Iron & Steelmaking Research Team, Technical Research Lab., POSCO, Pohang 790-785, Korea.

Manuscript submitted October 22, 2001.

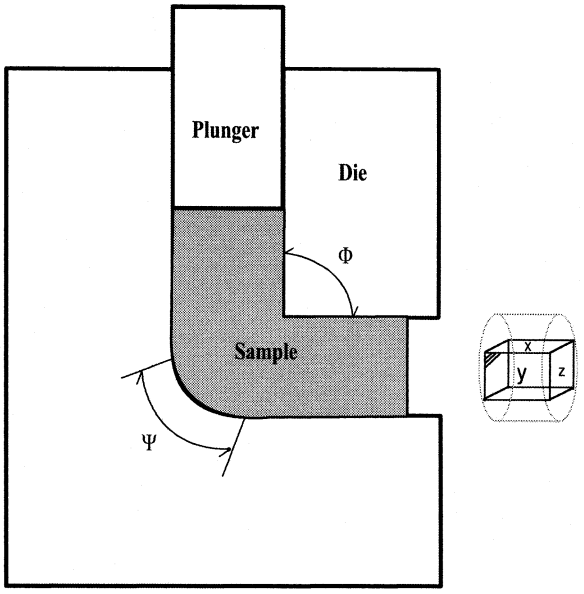


Fig. 1—Schematic illustration of die configuration for ECAP.

percent was solution treated at 803 K for 4 hours and then quenched into room-temperature water. The ECAP was conducted using a solid die made of SKD 61 with an internal angle ($\Phi$) of 90 deg between the vertical and horizontal channels and a curvature angle ($\Psi$) of 30 deg (Figure 1). For this die design, it has been shown that the effective strain accrued on a single pass through the die is $\sim$1.[11] Molybdenum disulfide ($MoS_2$) was used as lubricant. Rods with diameter of 17 mm and length of 100 mm were cut from the solid-solution-treated 6061 Al bar. They were held at 398 K for 20 minutes and then pressed through the die preheated to 398 K. Repetitive pressings of the same sample were performed up to 12 passes, giving a total strain of $\sim$12. All pressings were conducted by rotating each sample about the longitudinal axis by 90 deg in the same direction between consecutive passes (designated as route $B_c$[12]). After the ECA pressing, the rod was aged as a function of time at three different temperatures; 373 K, 413 K, and 448 K, to determine the optimum aging condition. Microhardness and tensile tests were carried out to evaluate the strength and ductility of the ECAP-processed materials. Vickers microhardness ($H_v$) was measured on the *y* plain (indicated in Figure 1), parallel to the longitudinal axes, by imposing a load of 100 g for 15 seconds. Tensile specimens of dog-bone geometry with the 5-mm gage length, 4-mm width, 2-mm thickness, and 2-mm shoulder radius with the gage length parallel to the longitudinal axis and with the width contained in the *y* plane were extracted from the center portion of the ECAP-processed materials by using electro-discharge machining. Tensile tests at room temperature were conducted at a fixed strain rate of $5 \times 10^{-4}$ $s^{-1}$ to examine strength and ductility. Tensile tests at elevated temperature (523 K and 813 K) were conducted in strain rate range between $1.7 \times 10^{-4}$ $s^{-1}$ and $1 \times 10^{-2}$ $s^{-1}$ to examine superplastic properties. All specimens were pulled on a tensile testing machine controlled under condition of cross-head speed. Tensile testing at elevated temperatures was carried out in air with the testing temperature continuously monitored and controlled to within $\pm$2 K of the desired value. The microstructures of the as–ECAP and post–ECAP aged samples were examined using a JEOL* transmission electron microscope (TEM). Samples for the TEM were cut from the *y* plane, ground to a thickness of $\sim$100 $\mu$m. Thin discs were electropolished in an electrolyte consisting of 15 pct nitric acid, 85 pct perchloric acid, and methanol at a temperature maintained between 233 and 243 K. Selected area electron diffraction (SAED) patterns were taken from areas having a diameter of $\sim$10 $\mu$m. The microstructure of the 12-pass material (post–ECAP aged) after superplastic deformation at 813 K and $\dot{\varepsilon} = 3 \times 10^{-4}$ $s^{-1}$ was examined optically after electrolytic polishing and etching (perchloric acid plus methanol, 16 V, 20 s).

*JEOL is a trademark of Japan Electron Optics Ltd., Tokyo.

## III. RESULTS AND DISCUSSION

### A. *Transmission Electron Microscope*

Figures 2 (a) through (d) exhibit a series of TEM bright-field images and the corresponding SAED patterns of solution-treated 6061 Al after (a) 1, (b) 4, (c) 8, and (d) 12 passes of ECAP, respectively. The grain size of the undeformed material determined by optics was as coarse as 40 to 80 $\mu$m. After one pass, elongated dislocation cells and subgrains have formed parallel to the shear direction. The size of the subgrains ranges from 0.2 to 0.4 $\mu$m and a high density of entangled dislocations is present inside a subgrain. Fine and equiaxed subgrains begin to be observed after four passes (Figure 2(b)). The average size of the subgrains (Figure 2(b)) is 0.3 to 0.4 $\mu$m, which is similar to its initial minimum shear band width. This result indicates that the equiaxed subgrains have formed through refinement of elongated subgrains by creation of additional boundaries in the band perpendicular to the long axis. This subgrain size retained up to pass 12. It is interesting to note that the grain size of 0.3 to 0.4 $\mu$m is very similar to those measured in the ECAP-processed peak-aged and overaged 6061 Al studied by Ferrasse *et al.*[7] This result implies that the minimum shear band width and size of subgrains formed during ECAP processing is little affected by the density and size of precipitate particles. The series of SAED patterns indicate that diffracted beam spots scatter more uniformly around rings as the pass number increases. This implies that the number of subgrains and the misorientation angle between subgrain boundaries increase with the pass number by forming new boundaries perpendicular to the shear direction and depositing new dislocations into existing subgrain boundaries. After eight passes, a further increase in misorientation angle is less clearly visible in the SAED pattern (Figure 2(d)).

### B. *Hardness*

The $H_v$ hardness of the solution-treated alloys is presented in Figure 3 as a function of ECAP pass number. A significant increase in hardness occurred (by about 55 pct) after a single pressing. Subsequent pressings increased the hardness further and the maximum was attained at four passes (by 85 pct). The large increase in the hardness during ECAP can be directly attributed to the considerable substructure refinement, which occurs during intensive plastic deformation. With further pressing, however, there is a gradual decrease

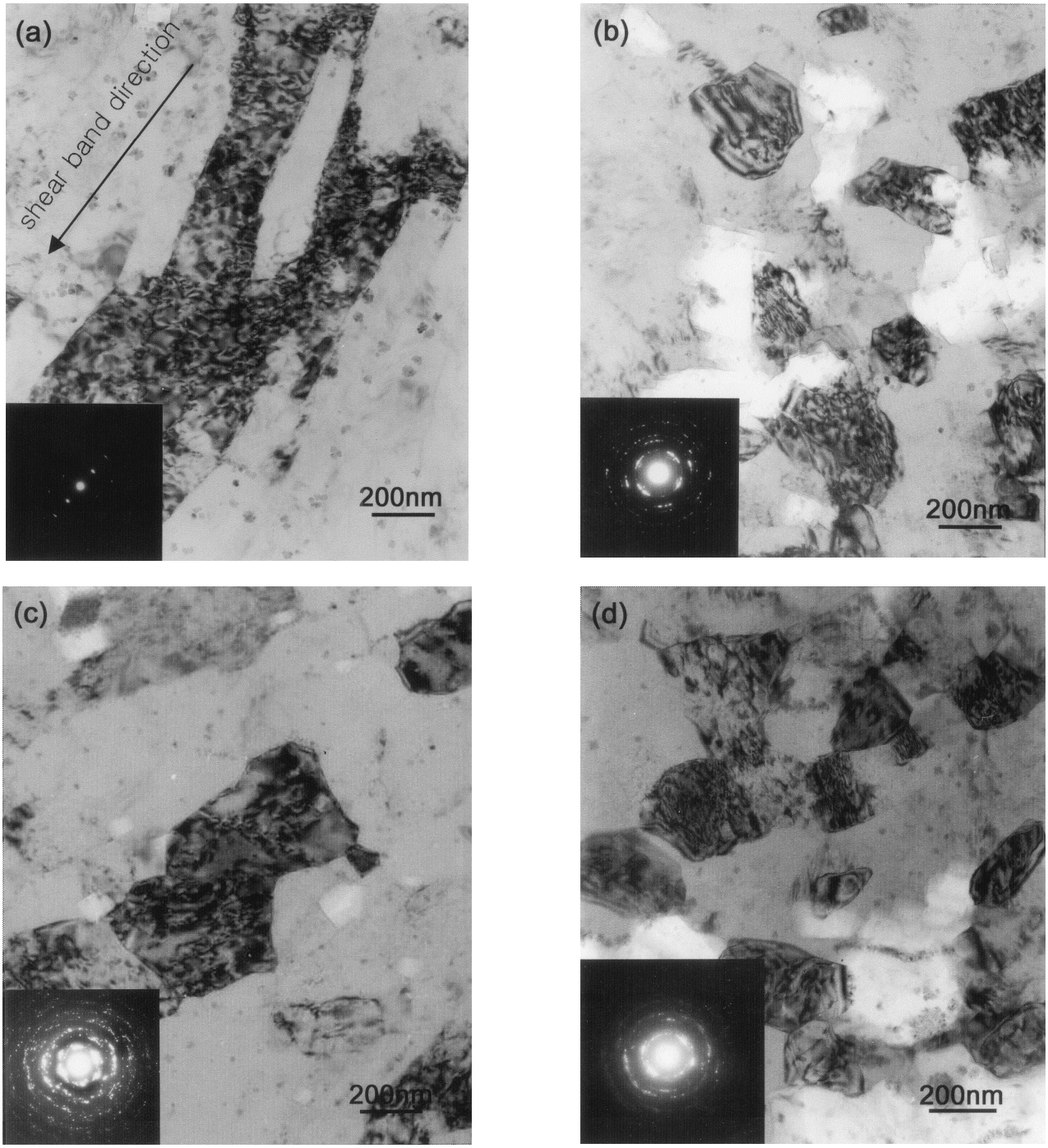


Fig. 2—TEM micrographs of the solid-solution-treated 6061 Al after ECAP processing to (*a*) 1 pass, (*b*) 4 passes, (*c*) 8 passes, and (*d*) 12 passes.

in the hardness. The ECAP-processed pure aluminum also shows a similar trend of decreasing hardness after the peak.[13] Chang *et al.*[14] reported that dislocation density in the grain interiors of a 1050 aluminum alloy decreases with the increase in strain and most of the grain interiors eventually become free of dislocations after a large deformation. The decrease in hardness after the peak, therefore, may be a result of a decreasing density of dislocations inside the subgrains.

It should be pointed out that some precipitation occurs during ECAP processing, preferentially on subgrain boundaries. This is illustrated in Figure 4. Therefore, one may consider the possibility of precipitation during ECAP processing as another mechanism for the strengthening obtained after ECAP. The contribution of this precipitation during ECAP process to the strengthening, however, seems to be relatively small compared with that of substructure refinement to the strengthening. This is because a similar extent of increase in hardness (by $\sim$ 100 pct) is observed in an ECAP-processed pure Al that is free of precipitates such that it is strengthened solely by substructure refinement.[13]

To increase the strength of the ECAP-processed materials further, a post–ECAP aging treatment was applied. Three aging-treatment temperatures were selected: 373, 413, and

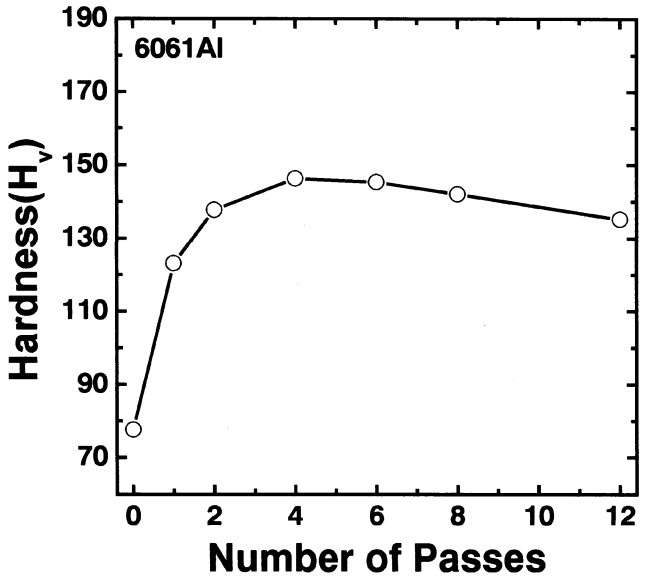


Fig. 3—Vickers hardness of ECAP-processed 6061 Al as a function of pass number.

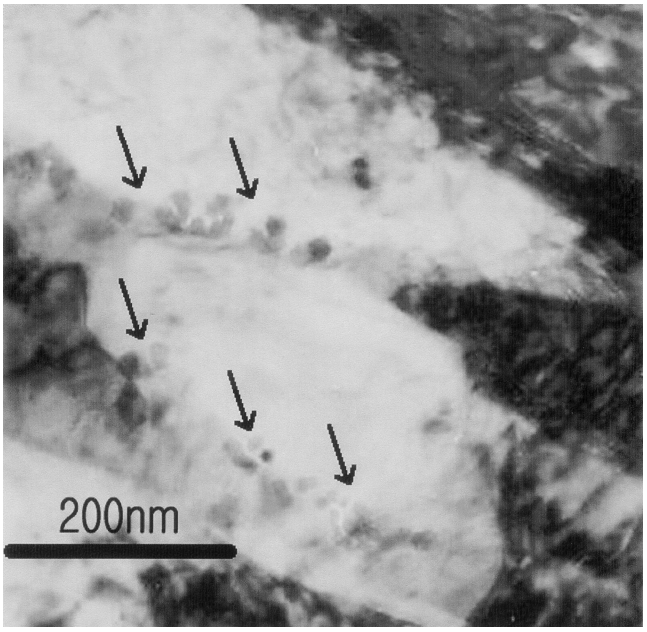


Fig. 4—A TEM micrograph of the two-pass 6061 Al. Some precipitates are observed on subgrain boundaries.

448 K. The hardnesses measured after aging at 448 K *vs* aging time (up to 8 hours*) are presented in Figure 5(a). In the unpressed material, as expected, there is an increase in hardness with aging time (50 pct after 8 hours). The pressed materials, on the other hand, exhibit the opposite trend. The hardness of one and two pass materials initially increases but starts to decrease after 1 hour. The materials pressed more than two times, on the other hand, show a decrease in hardness from the beginning. The decrease in hardness with time in the pressed material may indicate that the effect of recovery or grain coarsening[15] by annealing dominates the effect of precipitate hardening by aging. Indeed, the 12-pass material aged for 8 hours is found to have a larger grain size (1.3 $\mu$m) than the same material before aging (0.4 $\mu$m), though the former has a much higher density of second-phase particles. The observation of microstructural coarsening in the ECAP 6061 Al at a relatively low temperature may be primarily associated with the high driving force for coarsening due to the large stored deformation energy. The observed hardness increase in the one- and two-pass materials at the beginning of aging treatment, on the other hand, may suggest that the driving force for microstructural coarsening is not high enough due to the relatively low stored deformation energy after one or two passes. As the result the effect of precipitation hardening can dominate the effect of microstructural coarsening. After the T6 treatment, the pressed material ($H_v$ = 135) is harder than the unpressed material ($H_v$ = 115) at most by 15 pct. In this state, the advantage of ECAP processing is small.

*Aging at 448 K for 8 h is the peak aging condition (T6) for a 6061 Al.

To reduce the softening effect during aging, lower aging temperatures (413 and 373 K) were applied. Figure 5(b) shows the result of aging at 413 K on the hardness of the ECAP-processed alloys. When aged at 413 K, hardness gradually increases with aging time, becoming saturated at 4 hours or decreasing only slightly after that. The increment in strength, however, is rather small, except the one-pass material, where a relatively large hardening is observed. For aging at 373 K (Figure 5(c)), on the other hand, a noticeable increase in strength with aging time to 48 hours can be seen for all the materials (11 to 12 pct) irrespective of pass number. This result indicates that the age-hardening effect is predominant over the grain-coarsening effect at 373 K for up to 48 hours. Further aging, however, decreases the hardness (at 56 hours). The microstructure of the 12-pass material aged for 48 hours indicates (Figure 6(b)) that little grain growth has occurred during the aging treatment. At 373 K, the maximum hardness obtained after four passes is 160 $H_v$, which is a 40 pct increase in hardness compared to that of the T6-treated commercial 6061 Al (115 $H_v$). It is worthwhile to note that this increase is even larger than that (15 pct) obtained from the ECA-pressed 6061 Al with pre–ECAP peak-aging treatment.[7]

### C. *Microstructures after Aging*

Figures 6(a) and (b) are TEM micrographs for the 4- and 12-pass materials after aging at 373 K for 48 hours. It is apparent from the micrographs that density of precipitates has increased enormously after aging. Another observation is that the average particle size is larger in the 12-pass material than that in the 4-pass material. Figure 7 is a higher magnification of Figure 6(a) showing typical morphology of particles distributed over the matrix. Most particles have globular or spherical shape with 20 to 40 nm in diameter.

It is worthwhile to address here that the current particle morphology (globular or spherical) is different from that commonly observed in commercial aged 6061 Al alloys,[16–19] where spherical (or needle-shaped) (GP) zones, needle-shaped $\beta''$, rod-shaped $\beta'$, and disc-shaped $\beta$ particles have been observed. One of the controversies concerning the precipitation reactions in 6061 Al is whether the GP zones in this alloy system are spherical or needle shaped. Mondolfo[20] suggested that the precipitation sequence of GP zones begins with the formation of spherical zones that

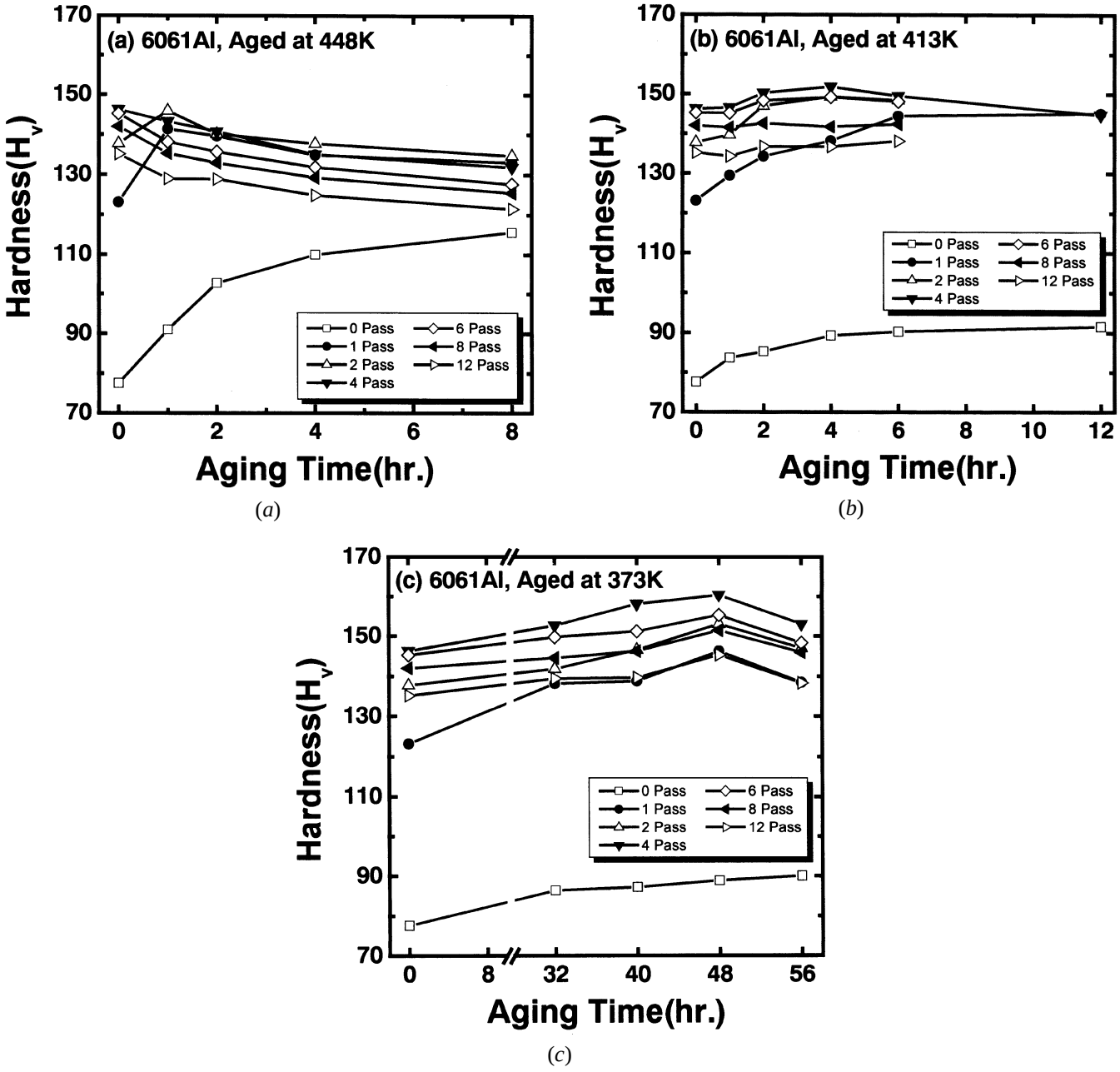


Fig. 5—Vickers hardness of the ECAP materials after aging at (*a*) 448 K, (*b*) 413 K, and (*c*) 373 K, as a function of aging time.

elongate along the cube matrix direction to assume a needle shape. The diameter of spherical zones was reported to be 5 nm. Note that most of the globular/spherical particles observed in the present alloy appear to be much larger than 5 nm. This result raises a possibility that precipitation behavior is modified in the presence of a heavily deformed microstructure. The formation of large spherical particles in the ECAP-processed material might be associated with increased diffusion from the high dislocation density generated during the ECAP procedure. Troeger and Starke[8] also observed spherodized particles rather than platelike particles in the 6013 Al rolled prior to aging. Enhanced diffusion may also explain the observed difference in particle size between the 4- and 12-pass materials (~20 nm *vs* 30 to 40 nm). As the 12-pass material has higher angle grain boundaries, more enhanced grain boundary diffusion is expected, and thereby particle growth is enhanced. A detailed analysis of the crystal structure and composition of the spherical precipitates is under study.

### D. *Tensile Behavior at Room Temperature*

The engineering stress-strain curves of the unpressed and ECAP materials without aging treatment are shown in Figure 8(a). The engineering stress-strain curves of the unpressed and ECA-pressed materials with aging treatments at 373 K for 48 hours are shown in Figure 8(b) for the purpose of comparison with Figure 8(a). Information regarding yield stress (YS), ultimate tensile strength (UTS), and tensile elongations of the unpressed and all the pressed materials are also summarized in Table I. As shown in Figure 8(a), YS and UTS continue to increase with pass number up to six

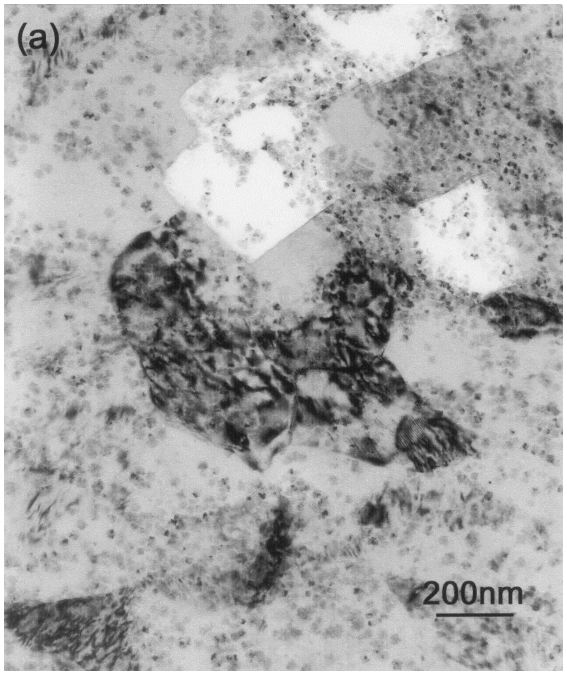


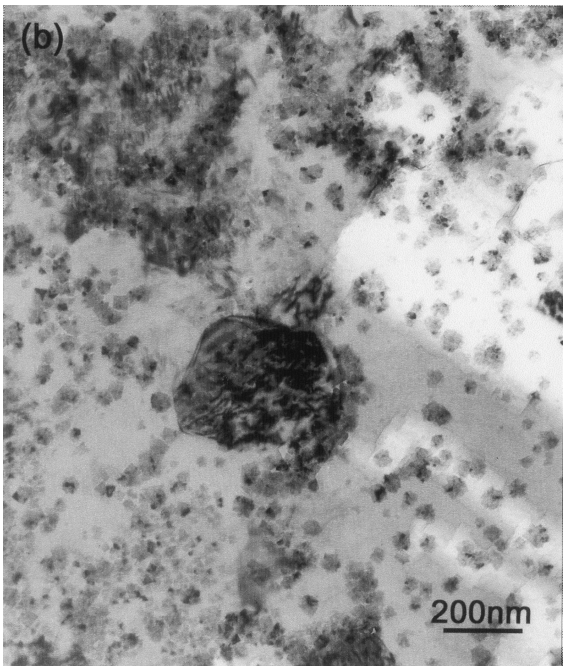


Fig. 6—TEM micrographs of the (*a*) 4-pass and (*b*) 12-pass material after aging treatment at 373 K for 48 h.

passes and then decrease gradually with further pressing. This result is consistent with the trend in hardness (Figure 3). The six-pass material shows the best result in strength improvement (YS = 410 MPa and UTS = 440 MPa). Tensile elongation, on the other hand, decreases by almost half after ECAP. This decrease in tensile ductility is directly attributable to the relatively small strain hardening after yielding in the ECAP-processed materials, which leads to a high sensitivity to strain localization in the form of necks.

The combination of the ECAP process with aging treatment at 373 K results in a further increase in YS and UTS of the pressed materials (Figure 8(b)), which is also in a good agreement with the trend of hardness data shown in Figure 5(c). The YS (427 MPa) and UTS (463 MPa) of the six-pass alloy with post–ECAP aging are higher than those (YS = 410 MPa; and UTS = 443 MPa) of the alloy without aging. Tensile elongation slightly decreased from 20 to 17 pct after post–ECAP aging. It is worthwhile to note that both the UTS strength (450 MPa) and the ductility (18 pct) of post–ECAP aged 6061 Al after four passes are greater than those of pre–ECAP peak-aged 6061 Al alloy (400 MPa and 13 pct)[7] with the same ECAP strain. The differences of strength and ductility may be linked with the difference in dislocation accumulation rate during ECAP processing and density of particles. The hardening rates of the underaged and solution-treated Al alloys were observed to be higher than those of peak-aged and overaged Al alloys by Hong *et al.*,[18,21] because dynamic recovery is suppressed by the high effective solute content in the matrix. Higher density of fine particles are present in the post-ECAP aged material than in the pre-ECAP aged material since heavily deformed microstructure provides a larger number of nucleation sites for precipitation. A pre–ECAP solid solution plus post–ECAP low-temperature aging treatment is, therefore, more effective in improving the strength of 6061 Al alloy than the pre–ECAP peak-aging treatment. Other advantages of the post–ECAP aging treatment over the pre–ECAP peak aging treatment are a lowering of the pressing load and the processing temperature for ECAP. This is because the solution-treated alloy has a lower strength and a larger ductility than the peak-aged material.

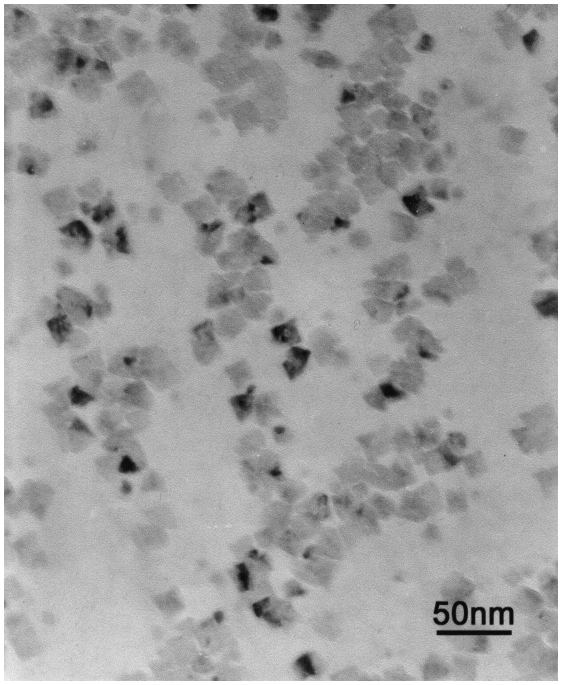


Fig. 7—A TEM micrograph of the (*a*) 4 pass after aging treatment at 373 K for 48 h, showing the typical morphology and size of particles distributed over the matrix.

### E. *Superplastic Behavior*

#### 1. *Low-temperature superplasticity*

Figure 9 shows the stress-strain curves obtained on the post–ECAP aged (373 K, 48 hours) alloys (0, 4, and 12

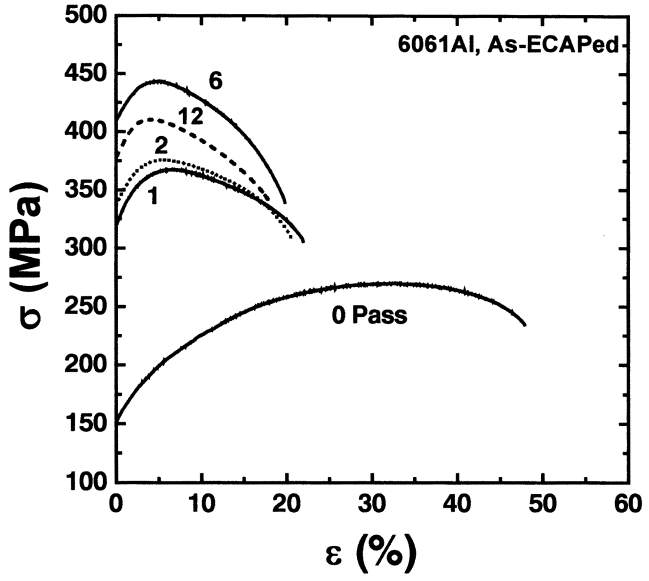


(*a*)

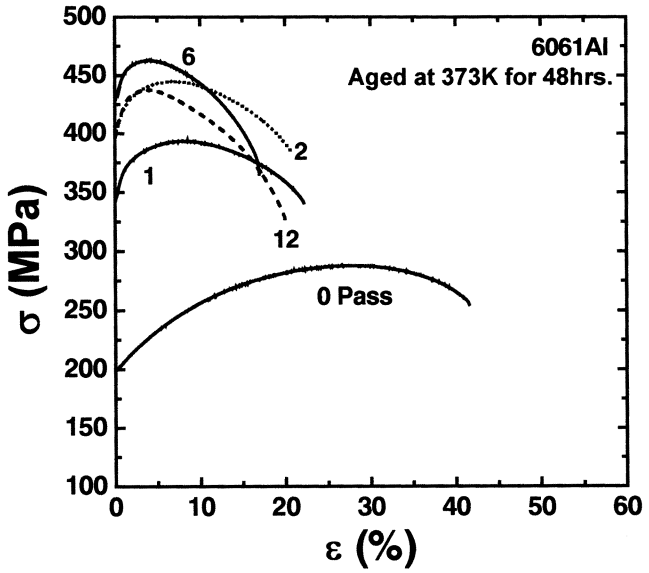


(*b*)

Fig. 8—The stress-strain curves for the ECAP-processed 6061Al alloy (*a*) without and (*b*) with a low-temperature aging treatment (373 K, 48 h).

passes) tested at 523 K and at $\dot{\varepsilon} = 1.7 \times 10^{-4}\ s^{-1}$. Tensile elongation of the ECAP materials increases with the pass number and is larger than that of the unpressed material. The ductility of 12-pass 6061 Al (155 pct) is much larger than that (20 pct) of the unpressed alloy. This low-temperature superplasticity, meaning large tensile elongations at temperatures considerably lower than the conventional temperature range for ordinary superplasticity, is often observed in ultrafine-grained metallic alloys and speculated to be related to enhanced diffusivity due to considerably increased grain boundary area by grain refinement.[22,23] The larger tensile elongation of the 12-pass material than that of the 4-pass material, despite the similarity in their grain sizes, may be attributed to easier grain boundary sliding due to higher grain boundary angles for the 12-pass material.

Another result to be noted in Figure 9 is that the flow

**Table I. Room-Temperature Mechanical Properties of ECAP Processed 6061 Al**

| Pass | Material | YS (MPa) | UTS (MPa) | Elongation (Pct) |
|---|---|---|---|---|
| 0 | as-pressed | 150.5 | 269.8 | 47.9 |
| | aged | 198.1 | 287.7 | 41.6 |
| 1 | as-pressed | 319.0 | 367.5 | 21.9 |
| | aged | 342.1 | 394.0 | 22.2 |
| 2 | as-pressed | 337.2 | 375.9 | 20.5 |
| | aged | 397.4 | 445.0 | 20.8 |
| 4 | as-pressed | 386.0 | 424.3 | 22.2 |
| | aged | 411.4 | 450.6 | 17.8 |
| 6 | as-pressed | 409.2 | 443.2 | 19.8 |
| | aged | 427.6 | 462.9 | 17.0 |
| 8 | as-pressed | 390.5 | 431.1 | 20.3 |
| | aged | 414.9 | 451.3 | 19.1 |
| 12 | as-pressed | 378.0 | 410.6 | 18.0 |
| | aged | 395.7 | 437.7 | 20.1 |

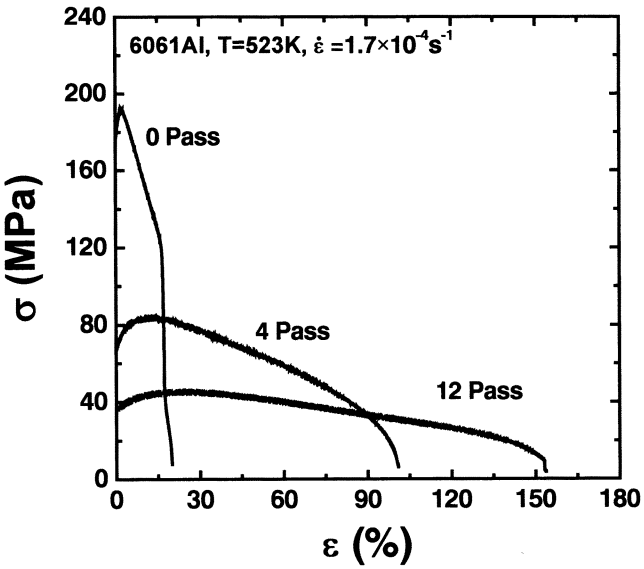


Fig. 9—The stress-strain curves obtained from the post–ECAP aged alloys tested at 523 K and at a strain rate of $1.7 \times 10^{-4}\ s^{-1}$.

stresses of the passed materials with finer grains are considerably lower than unpressed material with coarser grains. This observation suggests that grain boundary sliding is a dominant deformation mechanism for low-temperature superplasticity. To confirm this possibility further, a deformation mechanism map was constructed at 523 K. Figure 10(a) shows the deformation mechanism map for pure aluminum constructed at 523 K by using constitutive equations for various creep mechanisms developed either theoretically or phenomenologically. A full discussion on construction of this type of deformation mechanism map is available elsewhere.[24] It is evident from the map that datum points for the 4- and 12-pass materials are located in the $D_p$-controlled GBS (associated with $n = 4$, where $n$ is the stress exponent) and near the boundary between the $D_{gb}$-controlled GBS (associated with n = 2) and the $D_p$-controlled GBS, respectively. The datum point for the unpressed material (0 passes) is, on the other hand, located in the region where the $D_L$ controlled slip region (associated with $n = 7$) is

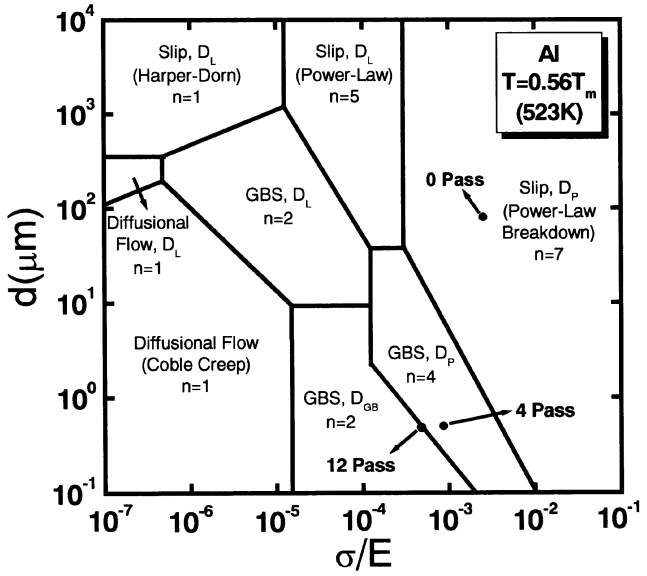


(*a*)

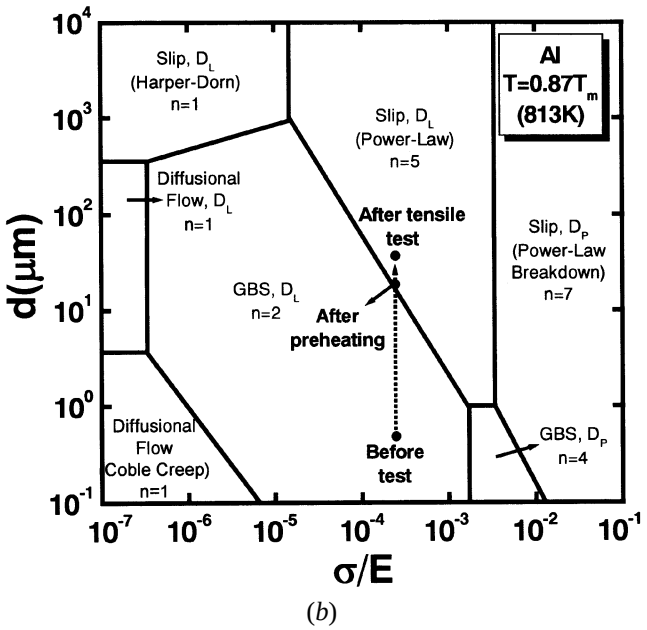


(*b*)

Fig. 10—Deformation mechanism maps constructed for pure Al at $T$ = (*a*) 0.56 $T_m$ and (*b*) 0.87 $T_m$. Here, $d$ is the mean grain size defined as $d = 1.74L$, where $L$ is the linear intercept grain size.

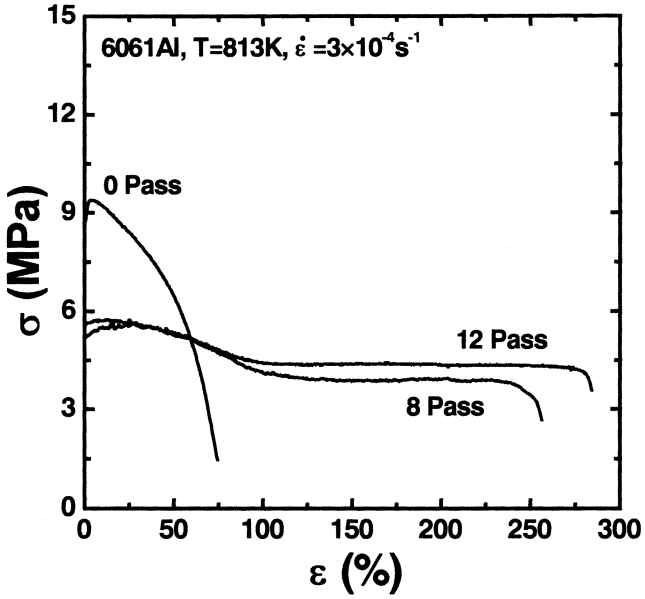


Fig. 11—The stress-strain curves obtained on post–ECAP aged (373 K, 48 h) alloys (0, 8, and 12 passes) tested at 813 K and at $\dot{\varepsilon} = 3 \times 10^{-4}$ s$^{-1}$.

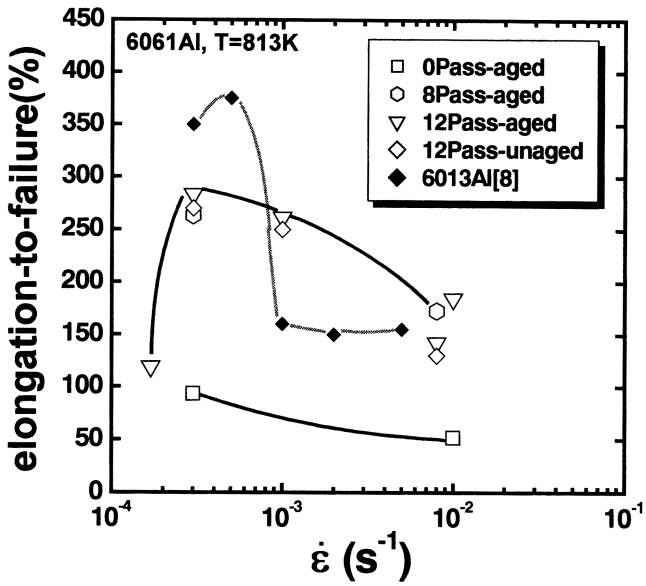


Fig. 12—The tensile elongations for the 8- and 12-pass 6061 Al (post–ECAP aged at 373 K for 48 hours.) and 6013 Al[8] as a function of strain rate at 813 K.

predicted to govern the plastic flow. This result suggests that the rate-controlling process for the low-temperature superplasticity observed in the 12-pass material is either $D_{gb}$-controlled GBS or $D_p$-controlled GBS.

2. *Superplasticity at elevated temperatures*

Figure 11 shows the stress-strain curves obtained on the post–ECAP aged (373 K, 48 hours) alloys (0, 8, and 12 passes) tested at 813 K and at $\dot{\varepsilon} = 3 \times 10^{-4}$ s$^{-1}$. Tensile elongations after 8 and 12 passes, which are similar, are 250 to 280 pct. Figure 12 is the plot of tensile elongation *vs* strain rate at 813 K for the 8- and 12-pass materials. Tensile-elongations over 250 pct were obtained at strain rates as high as $1 \times 10^{-3}$ s$^{-1}$ in these materials. The linear intercept grain size of the 12-pass material is 18.5 $\mu$m after the elongation-to-failure test at 813 K and at $\dot{\varepsilon} = 3 \times 10^{-4}$ s$^{-1}$ (Figure 13(a)). To check whether this large grain growth occurred during the preheating period before the initiation of the elongation-to-failure test or during the elongation-to-failure test, grain coarsening during the preheating period was investigated. The 12-pass material was heated in a preheated furnace for 10 minutes and then cooled rapidly before microstructural observation. The 10 minute heating refers to the preheating period. The mean grain size of the rapidly cooled sample was determined to be 11.4 $\mu$m (Figure 13(b)). Therefore, it is apparent that significant grain coarsening occurs during the preheating stage.

It is worthwhile to note that the ECAP alloy (12 pass) without the post–ECAP aging treatment also shows a similar

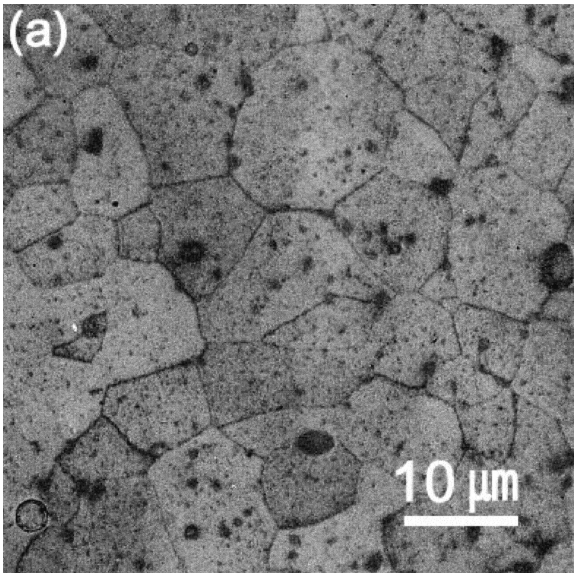


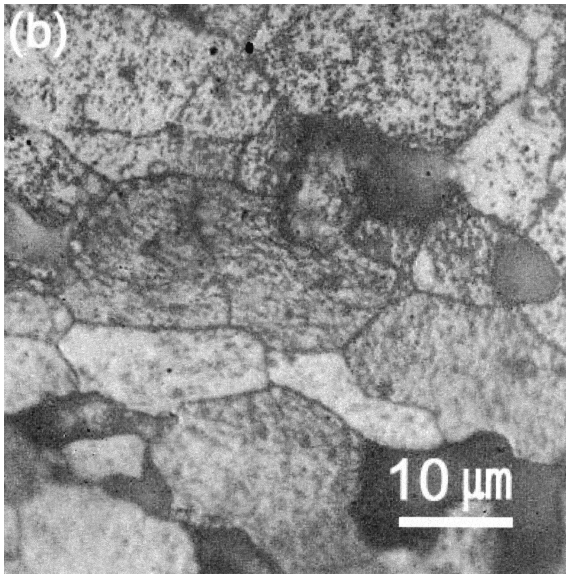


Fig. 13—Optical microstructures of the 12-pass material tested at 813 K and at $\dot{\varepsilon} = 3 \times 10^{-4}\ s^{-1}$: (*a*) after preheating and (*b*) after elongation-to-failure test.

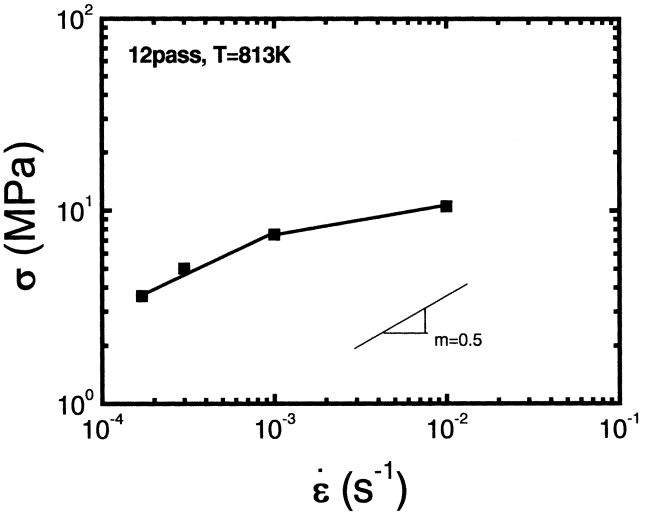


Fig. 14—The strain rate *vs* flow stress curve at 813 K for the 12-pass material post–ECAP aged at 373 K for 48 h.

amount of tensile elongation. This result implies that the particles created during aging treatment do not play an important role in improving tensile ductility, probably because the particles are not large and stable enough at high temperatures to suppress grain growth effectively. Nevertheless, the present study suggests that high-temperature ductility can be significantly improved through ECAP processing. Superplasticity has never been observed in ingot-processed 6061 Al. Indeed Kovacs-Csetenyi *et al.*[10] reported that 6061 Al was not superplastic between 773 and 843 K and the strain rate sensitivity was 0.16. They observed superplasticity in 6xxx Al alloys with high contents of Cu or transition metals.[10] Their observation is compatible with the result of Troeger and Starke that superplasticity is observed in 6013 Al with a higher Cu content. It is interesting to note that, at the strain rate of $10^{-3}\ s^{-1}$ and at 813 K, the 6061 Al of the present study (260 pct) exhibits a larger tensile elongation than the 6013 alloy (160 pct) in which the microstructure was stabilized by distribution of overaged globular precipitates with near 1-$\mu$m diameter.

The variation of strain rate as a function of flow stress measured at a fixed strain of 0.1 in the flow stress-strain curves for the aged 12-pass material at 813 K is shown in Figure 14. The slope of the curve, indicating the strain-rate-sensitivity exponent, $m$, exhibits $m \approx 0.5$ up to the strain rate of $10^{-3}\ s^{-1}$, corresponding to the dominant deformation mechanism of GBS. The deformation mechanism map at 813 K shown in Figure 10(b) indicates that the dominant deformation process for the 12-pass material at $\dot{\varepsilon} = 3 \times 10^{-4}\ s^{-1}$ changes from a $D_L$-controlled GBS to $D_L$-controlled slip process during course of the tensile testing due to considerable grain growth. Note that the state of material is near the border between the two deformation mechanisms only after the pre-heating. This may be one of the reasons why marginal superplasticity is observed in this material despite its grain size, which is very fine initially. If the particle nucleation stimulation method[8] is adopted in the ECAP 6061 Al alloy to introduce a high density of overaged globular precipitates, which are expected to suppress large grain growth during the preheating stage and deformation at elevated temperatures, a better result in superplasticity may be obtained. Such an effort is now in progress.

## IV. SUMMARY AND CONCLUSIONS

In this study, a post–ECAP low-temperature aging treatment is found to significantly enhance the strength of a cast 6061 Al. Before the ECAP process, the alloy was solution treated and quenched into water, and after ECAP processing, the material was aged at relatively low temperatures. The best result in room-temperature strength was found when the six-pass material was aged at 373 K for 48 hours. A large increase of ~45 pct in UTS and YS is obtained in the post–ECAP aged material (six passes) compared to the peak-aged (T6) commercial 6061 Al alloy. The 8- and 12-pass materials with very fine grains and fairly high-angle grain boundaries exhibit low-temperature superplasticity and reasonable superplasticity at elevated temperatures.

## ACKNOWLEDGMENTS

This work was supported by Grant No. 2000-1-30100-013-3 from the Basic Research Program of the Korea Science & Engineering Foundation.

## REFERENCES

1. R.S. Mishra, R.Z. Valiev, S.X. McFadden, and A.K. Mukherjee: *Mater. Sci. Eng. A*, 1998, vol. A252, pp. 174-78.
2. R.Z. Valiev, A.V. Kornikov, and R.R. Mulyokov: *Mater. Sci. Eng. A*, 1993, vol. A168, pp. 141-48.
3. M. Furukawa, Y. Ma, Z. Horita, M. Nemoto, R.Z. Valiev, and T.G. Langdon: *Mater. Sci. Eng. A*, 1998, vol. A241, pp. 122-28.
4. P.B. Berbon, N.K. Tsenev, R.Z. Valiev, M. Furukawa, Z. Horita, M. Nemoto, and T.G. Langdon: *Metall. Mater. Trans. A*, 1998, vol. 29A, pp. 2237-43.
5. Y. Iwahashi, Z. Horita, M. Nemoto, and T.G. Langdon: *Acta Mater.*, 1998, vol. 46, pp. 3317-31.
6. R.Z. Valiev, N.A. Krasilnikov, and N.K. Tsenev: *Mater. Sci. Eng. A*, 1991, vol. A137, pp. 35-40.
7. S. Ferrasse, V.M. Segal, K.T. Hartwig, and R.E. Goforth: *J. Mater. Res.*, 1997, vol. 12, pp. 1253-61.
8. L.P. Troeger and E.A. Starke Jr: *Mater. Sci. Eng. A*, 2000, vol. A277, pp. 102-13.
9. W.J. Kim, S.H. Hong, and J.H. Lee: *Mater. Sci. Eng. A*, 2001, vol. A298, pp. 166-73.
10. E. Kovacs-Csetenyi, T. Torma, T. Turmezey, N.Q. Chinh, A. Juhasz, and I. Kovacs: *J. Mater. Sci.*, 1992, vol. 27, pp. 6141-45.
11. Y. Iwahashi, J. Wang, Z. Horita, M. Nemoto, and T.G. Langdon: *Metall. Mater. Trans. A*, 1996, vol. 29A, pp. 2245-52.
12. M. Furukawa, Y. Iwahashi, Z. Horita, M. Nemoto, and T.G. Langdon: *Mater. Sci. Eng. A*, 1998, vol. A257, pp. 328-32.
13. Y. Iwahashi, Z. Horita, M. Nemoto, and T.G. Langdon: *Acta Mater.*, 1997, vol. 45, pp. 4733-41.
14. C.P. Chang, P.L. Sun, and P.W. Kao: *Acta Mater.*, 2000, vol. 48, pp. 3377-85.
15. M. Furukawa, Y. Iwahashi, Z. Horita, M. Nemoto, N.K. Tsenev, R.Z. Valiev and T.G. Langdon: *Acta Mater.*, 1997, vol. 45, pp. 4751-57.
16. G. Thomas: *J. Inst. Met.*, 1961-62, vol. 90, p. 57.
17. W.F. Smith: *Metall. Trans.*, 1973, vol. 4, pp. 2435-40.
18. S.I. Hong, G.T. Gray III, and Z. Wang: *Mater. Sci. Eng. A*, 1996, vol. A221, pp. 38-47.
19. H. Cordier and W. Gruhl: *Z. Metallkd.*, 1965, vol. 56, p. 669.
20. L.F. Mondolfo: *Aluminum Alloys: Structure and Properties*, Butterworth and Co., London, 1976, p. 566.
21. S.I. Hong, G.T. Gray III, and J.J. Lewandowski: *Acta Metall. Mater.*, 1993, vol. 41, p. 2337.
22. M. Mabuchi, K. Ameyama, H. Iwasaki, and K. Higashi: *Acta Mater.*, 1999, vol. 47, pp. 2047-57.
23. K. Neishi, T. Uchida, A. Yamauchi, K. Nakamura, Z. Horita, and T. G. Langdon: *Mater. Sci. Eng. A*, 2001, vol. A307, pp. 23-28.
24. O.A. Ruano, J. Wadsworth, and O.D. Sherby: *J. Mater. Sci.*, 1985, vol. 20, p. 3735.